*International Journal of Interdisciplinary Innovative Research &Development (IJIIRD)*
**ISSN: 2456-236X**
Vol. **05** Special Issue **01** | **2020**

# MMC-Based SRM Drives for Hybrid-EV with Decentralized BESS configured in Battery Driving Mode

[1]Shweta Puntambekar, [2] Mugdha Shimpi

[1,2] *Assistant Professor Department of Electrical Engineering, Zeal College of Engineering and Research Savitribai Phule Pune University, Pune*

**ABSTRACT**

**With clean energy requirements in urban transportations, electric vehicles (EVs) and hybrid EVs (HEVs) have received much attention owing to their fuel-efficient performance and protection of the environment against exhaust emission, which have been significantly supported all over the world.**

**A modular multilevel converter (MMC) based switched reluctance motor (SRM) drive with decentralized battery energy storage system for hybrid electric vehicle applications is seen as an efficient system in hybrid vehicle mobility. In this drive, battery cell and half-bridge converter is connected as a sub-module (SM), and multiple SMs are connected together for the MMC. Flexible charging and discharging functions for each SM are obtained by controlling switches in SMs. Compared to conventional and existing SRM drives; there are several advantages of this topology. The functioning of the drive is effectively simulated in MATLAB and performance is evaluated. In the proposed MMC-based SRM drive, battery driving mode and generator control unit (GCU) driving mode, GCU- battery driving mode are tested.**

**Keywords: Electric Vehicles, Modular Multilevel Converter, Switched Reluctance Motor, Charging-Discharging**

## 1. INTRODUCTION

The world is having a shift from conventional fuel vehicles to Electric Vehicles. The Electric mobility technologies are evolving very fast with rapid system implementation. In Hybrid Electric Vehicle (HEV), power train systems, permanent magnet motors are popular due to high torque and high efficiency.[1] The permanent magnet is expensive and decreases the motor reliability and performance in high- temperature and high-speed operations[2]. Another option used is Switched reluctance motors (SRMs), which are known to have a more robust structure due to no rotor windings and permanent magnets, which can provide a more low-cost topology and a longeroperation time in high-temperature environments[3]. Also, they have a much wider speed range compared to that of other motors, which is very important for electric power-trains. Because of further advantages such as high torque, simple structure, high reliability, and excellent fault-tolerance ability, SRMs have become a promising solution for power-train systems. 3-phase full-bridge converters are used for SRM drives to achieve modular topology.[4] An asymmetric three-level neutral point diode-clamped converter is proposed to reduce the torque ripple and improve the system efficiency.[5] A dual supply buck–boost converter is introduced for SRM drives to provide soft starting, reduce the torque ripple, and improve the power density.[6] A quasi-Z source integrated converter is designed, which can reduce the DC-link capacitance and extend the speed range.[7] Multilevel converters are developed to improve the phase voltage in the winding excitation and demagnetization regions to reduce the current rising and falling times for high-speed operations.[8]

For EVs/HEVs, the wide operational speed, torque demand, and integrated converter functions in vehicular applications pose challenges to the traction system design. A motor drive system can be used for driving a traction motor as well as for charging the battery.[9] The overall efficiency of the electrified traction drive can be improved due to the single conversion stage between the battery and the motor.[10] A split converter for four-phase SRMs is suggested for EVs, and a central-tapped winding node is used to connect the phase windings and converter circuit, where on-board charging is achieved.[11] A C-dump converter can be used with integrated charging capability. SRM drives with a front-end dc–dc converter helps to obtain variable dc- bus voltage and battery charging ability, while the additional use of inductors and capacitors reduces the power density, and the modular structure and flexible battery fault-tolerance ability are not achieved.[12]

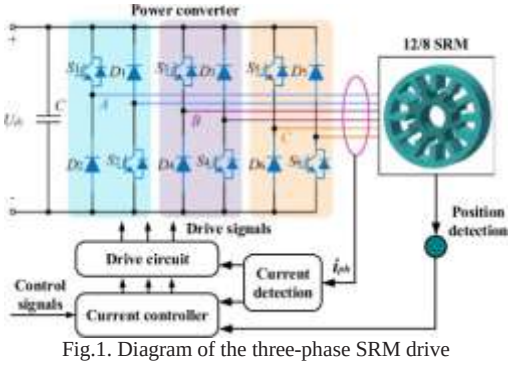


Fig.1. Diagram of the three-phase SRM drive

The advantages of the topology are as follows:

| |
|---|
| Multiple working modes can be flexibly selected by controlling the MMC and full-bridge converter. |
| The MMC-based topology can drive the SRM from variable dc voltages according to the running speed to reduce the voltage stress on the switches which also improves the reliability. |
| Multilevel phase voltage is achieved due to additional battery charging under running conditions, which improves the torque capability. |
| By using standard half-bridge modules for both the MMC and full-bridge converter, completely modular topology is achieved. |
| Flexible charging functions can be directly achieved through the proposed drive without external ones, including the running charging and standstill charging modes. |
| Flexible fault-tolerance ability for each battery cell is equipped by easily bypassing the faulty one. |
| The battery state-of-charge (SOC) can be balanced by controlling the SM charging according to the SOC level. |

Fig.2. Advantages of MMC Configuration

Due to the highly modular structure, multilevel voltage, and inherently bidirectional characteristic, modular multilevel converters (MMCs) have been employed for ac machines to improve sinusoidal waveforms for performance enhancements.[13] Multilevel converter topologies have been investigated for SRMs to enhance the torque capability, improve the high-speed performance, and reduce the power loss for high speed and high-power applications.[14] By developing the MMC topology for SRM drives, the torque can be improved due to the multilevel voltage, the voltage stress on the switches can be reduced with flexible dc-bus voltage.

## 2. CASCADED H-BRIDGES MULTILEVEL INVERTER

A 1-phase structure of an m-level cascaded inverter is seen in figure below. Each separate DC source isconnected to a single-phase full-bridge, or H-bridge, inverter.[15] Each inverter level can generate three different voltage outputs, +Vdc, 0, and –Vdc by connecting the dc source to the ac output by different combinations of the four switches, S1, S2, S3, and S4. To obtain +Vdc, switches S1 and S4 are turned on, whereas –Vdc can be obtained by turning on switches S2 and S3. By turning on S1 and S2 or S3 and S4, the output voltage is 0. The ac outputs of each of the different full-bridge inverter levels are connected in series such that the synthesized voltage waveform is the sum of the inverter outputs. The number of output phase voltage levels m in a cascade inverter is defined by m = 2s+1, where s is the number of separate dc sources.

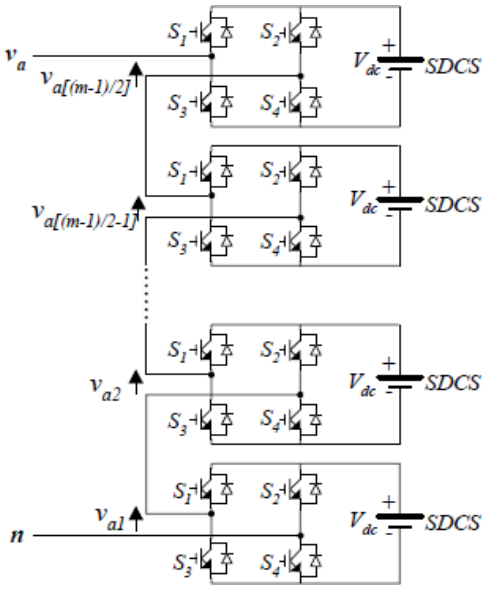


Fig.3.Single-phase structure of a multilevel cascaded H-bridges inverter [16]

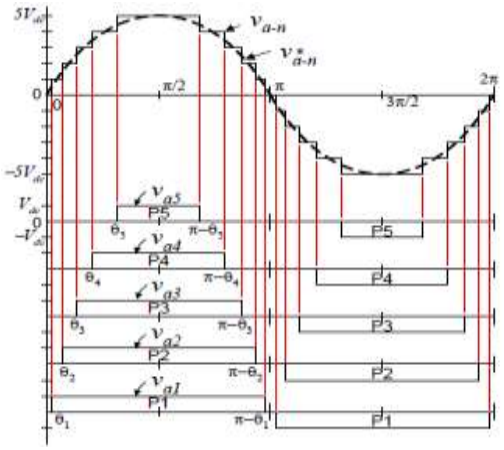


Fig.4.Output phase voltage waveform of an 11-level cascade inverter with 5 separate dc sources. [18]

The main advantages of multilevel cascaded H- bridge converters are as follows [17]:

*Advantages:*

- The number of possible output voltage levels is more than twice the number of dc sources (m=2s+ 1).
- The series of H-bridges makes for modularized layout and packaging. This will enable the manufacturing process to be done more quickly and cheaply.

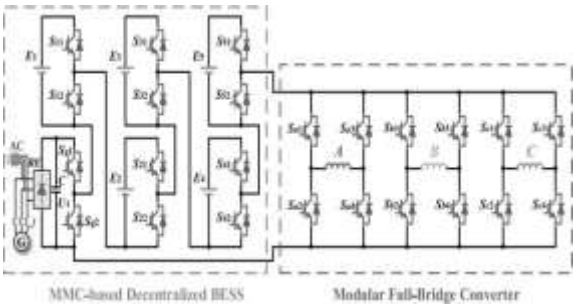


Fig.5.MMC-based SRM drive with six SMs for HEVs

## 3. METHODOLOGY

Figure above shows the MMC with decentralized BESS. A half-bridge converter and a battery pack Ex are employed as an SM, and each SM is made up of two insulated-gate bipolar transistors (IGBTs), including an upper switch Sx1 and a lower switch Sx2. The output voltage of each SM is $U_{SM}$, which is determined by the SM working state according to the ON–OFF state of two switches, and multiple SMs are connected in series to

form a decentralized BESS for the total dc-bus voltage $U_{dc}$. In this configuration, battery cells are decentralized by individual SMs and each battery cell SM can be controlled independently. As shown in Fig. 4, each SM is a two-level half- bridge converter consisting of a battery cell and two switches. In the IGBT, there is an integrated anti- parallel diode. The state of the anti-parallel diode is defined as ON when there is a current flowing through it, and is defined as OFF with no current. The operation states of the two-level SM under different IGBT switching states are shown in Fig. 4 and Table I.

TABLE I: SM OPERATION STATES

| SM state | $S_{x1}$ | $S_{x2}$ | $D_{x1}$ | $D_{x2}$ | $U_{cm}$ | $i_{arm}$ | $E_x$ |
|---|---|---|---|---|---|---|---|
| On | On | Off | Off | Off | $U_{by}$ | Positive | Discharging mode |
| On | Off | Off | On | Off | $-U_{by}$ | Negative | Charging mode |
| Off | Off | On | Off | Off | 0 | Negative | Bypass mode 1 |
| Off | Off | Off | Off | On | 0 | Positive | Bypass mode 2 |

SRM drive with six SMs for HEV applications, including an MMC-based decentralized BESS and a modular full-bridge converter. The full-bridge converter is used to achieve a completely modular converter structure, where the commercial power modules can be directly used for the proposed drive, which is beneficial for the market. The MMC is composed of six SMs by using IGBTs with integrated fast recovery anti-parallel diode, an energy storage unit including five battery packs (E1–E5), and a GCU including a generator (G), a relay (J), a rectifier (RE), and a capacitor (C). In the modular full-bridge converter, six half-bridge modules are used to drive the three-phase SRM, where two half-bridge modules are employed for one phase, which achieves a completely modular structure for massive production. By employing the proposed SRM drive, multiple working modes can be flexibly achieved and the system performance can be improved.

## 4. BATTERY DRIVING MODE OF BESS

*1) Full Battery Cells Driving*- When relay J is OFF and switches Sg2 is ON, the GCU SM is bypassed and the proposed SRM drive can work in pure- battery driving mode. Under this condition, the dc- bus voltage can be flexibly controlled by employing different SMs. Fig. 6 shows the working stages of the motor drive in battery driving mode with flexible excitation and demagnetization voltages. Fig. shows the condition that E1–E5 are all employed for excitation, where switches S11, S21, S31, S41, and S51 are all turned ON, and S12, S22, S32, S42, and S52 are all kept OFF for the phase winding excitation; in the winding demagnetization mode, the current flows back to the power source through S11, S21, S31, S41, and S51. The phase A voltage is directly the dc-bus voltage under this condition, which can be expressed as

$$U_a = \begin{cases} 5U_{\mathrm{SM}}, & \text{Phase A excitation} \\ -5U_{\mathrm{SM}}, & \text{Phase A demagnetization.} \end{cases}$$

*2) Two Battery Cells Driving With Two Additional Battery Cells Charging:*
Figure shows the conditions that two battery cells are employed for the winding excitation, and additional two SMs are employed to improve the voltage for winding demagnetization and achieve battery charging during running conditions. For example, $E_1$ and $E_2$ are used to supply the power to the motor, and $E_3$ and $E_4$ are employed to increase the demagnetization voltage, where $S_{11}$ and $S_{21}$ are bothturned ON, and $S_{52}$ is also turned ON to bypass the E5 SM. In the excitation mode of phase A, the current flows through S11 and S21, the diodes in S32 and S42, and the bypass switch S52 to the phase A converter, as shown in Fig. 6(c); when phase A is turned OFF, the demagnetization current goes through the bypass switch S52, the diodes in S31 and S41, and switches S11 and S21 to the power source. The demagnetization voltage is elevated by E3 and E4, where the multilevel phase voltage can be achieved to accelerate both the excitation and demagnetization processes for torque improvements, and also E3 and E4 can be charged by the demagnetization current. Under this condition, the charging and discharging voltages for the dc link are given by:

$$U_{\mathrm{dc}} = \begin{cases} 2U_{\mathrm{SM}}, & \text{Discharging state} \\ 4U_{\mathrm{SM}}, & \text{Charging state.} \end{cases}$$

The phase A demagnetization voltage is directly increased to $-4U_{SM}$ due to additional battery cells charging. Although the dc-bus voltage is only $2U_{SM}$ in the discharging mode, the excitation voltage of phase A can still be elevated to $4U_{SM}$ by phase C demagnetization, according to the current overlapping states. When the phase C current is larger than the phase A current in the phase C demagnetization stage, the phase C winding works as a current source to supply the current to phase A and simultaneously charge the battery. Because the phase C winding is under the demagnetization voltage
$-4U_{SM}$ due to the battery cell E3 and E4 charging, the phase A voltage can be elevated to $4U_{SM}$ when the phase C winding supplies the current to phase A.

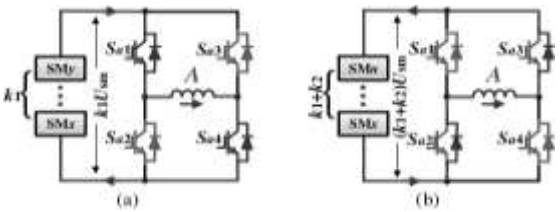


Fig.6. Battery driving mode with flexible multilevel voltage and battery charging. (a) Excitation. (b) Demagnetization and battery charging.

When the phase C current decreases to be smaller than phase A current, the dc-link power source and phase C both supply the current to phase A, and the phase A voltage returns to $2U_{SM}$. Hence, after the excitation current quickly established at the beginning of the turn-ON region with an increased voltage, the phase voltage can immediately decrease to the power supply voltage in the main turn-ONregion, which not only improves the torque, but also achieves a lower excitation voltage.

## 5. SIMULATION VERIFICATION

To verify the effectiveness of the proposed MMC- based SRM drive, experiments are carried out on a scale-down three-phase 12/8 SRM prototype by employing six SMs for proof of concept. Table I gives the main parameters of the SRM. A proportional integral controller is employed to implement the closed-loop speed control and the current hysteresis control method is used for phase current regulation. A multichannel isolated oscilloscope is employed to observe the voltage and current waveforms. In the motor test bed, a Parker ac servomotor is used as the load, which can be controlled by a load controller inside the cabinet. A 3-DOF bracket can be adjusted to ensure a balanced connection between the SRM and the load motor. A high-precision torque sensor (Lorenz 0261Due) is used to detect the instantaneous output torque. A 2500-line incremental encoder (ZZU4809) is installed on the motor bearing to detect the rotor position and calculate the rotational speed. A programmable dc power source is utilized to simulate the GCU part. Five 24-V battery packs are employed for the MMC configuration.

Table Ii: Motor Parameters

| S. No. | Parameters | Value |
|---|---|---|
| 1 | Phase No. | 3 |
| 2 | Stator/rotor poles | 12/8 |
| 3 | Rated power(W) | 750 |
| 4 | Rated Speed(r/min) | 1500 |
| 5 | Phase resistance(ohm) | 3.01 |
| 6 | Min. phase inductance(mH) | 27.2 |
| 7 | Max. phase inductance(mH) | 256.7 |
| 8 | Rotor Outer Diameter (mm) | 55 |
| 9 | Rotor Inner Diameter (mm) | 30 |
| 10 | Stator Outer Diameter (mm) | 102.5 |
| 11 | Stator Inner Diameter (mm) | 55.5 |
| 12 | Stack Length (mm) | 80 |
| 13 | Stator Arc Angle (deg) | 14 |
| 14 | Rotor Arc Angle (deg) | 16 |

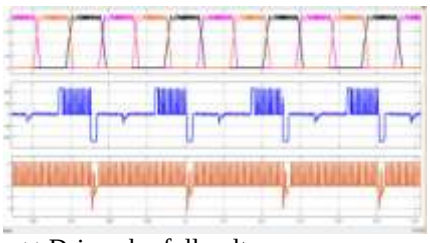

(a) Driven by full voltage.

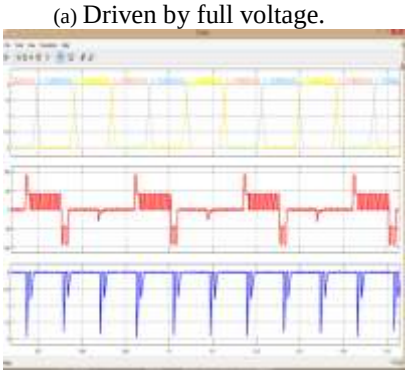

(b) Driven by E1 and E2 with E3 and E4 charging

(c) Driven by E1 with E2 and E5 charging. Fig.7. Battery driving mode at low speed

Figure shows the experimental waveforms in the battery driving mode at low speed of 300 r/min and 2-N·m load, where $i_a$, $i_b$, and $i_c$ are the currents of phases A, B, and C, respectively, $U_a$ is the phase A voltage, $i_{by}$ is the battery current flowing through full cells, and $i_{byx}$ is the battery current flowing through cell x. When all the battery cells are put into use, the excitation and demagnetization voltages on the phase winding are both the full-battery voltage, and the battery cells are charged and discharged alternately in each current period, as shown in Fig. 14(a). When parts of the battery cells are employed as a lower voltage power supply, the motor drive can work under multilevel phase voltage by additional battery charging during the demagnetization process, where running charging is achieved. As shown in Fig. 14(b), E1 and E2 are employed to supply the power, and E3 and E4 are used for additional charging.

The demagnetization voltage of phase A is directly elevated by E3 and E4 charging; the excitation voltage of phase A is also increased in phase A and phase C current overlapping region, when the demagnetization current of phase C is larger than the excitation current of phase A. Due to the multilevel voltage, the excitation and demagnetization processes are both accelerated. Battery cells E3 and E4 are charged by the demagnetization current of each phase. In Fig. 14(c),E1 is employed as the power supply, and E2 and E5 are used for additional charging, where multilevel phase voltage is also achieved. Therefore, in the battery driving mode, the dc-bus voltage can be flexibly changed according to the requirement, the voltage stress on the switches can be dramatically reduced, and the battery cells can be flexibly selected for additional charging during the demagnetization process according to the SOC level. Hence, the energy can be transferred among the battery cells to achieve the SOC balance.

## 6. CONCLUSION

A modular multilevel converter (MMC) based switched reluctance motor (SRM) drive with decentralized battery energy storage system for hybrid electric vehicle applications is seen as an efficient system in hybrid vehicle mobility. In this drive, battery cell and half-bridge converter is connected as a sub-module (SM), and multiple SMs are connected together for the MMC. Flexible charging and discharging functions for each SM are obtained by controlling switches in SMs. Compared to conventional and existing SRM drives; there are several advantages of this topology. A lower dc-bus voltage can be flexibly achieved by selecting SM operation states, which can dramatically reduce the voltage stress on the switches. Multilevel phase voltage is obtained to improve the torque capability. Battery state-of-charge balance can be achieved by independently controlling each SM. Flexible fault- tolerance ability for battery cells are equipped. The battery can be flexibly charged under both running and standstill conditions. Furthermore, a completely modular structure is achieved by using standard half- bridge modules, which is beneficial for market mass production.

## 7. REFERENCES

[1] S. S. Williamson, A. K. Rathore, and F. Musavi, “Industrial electronics for electric transportation: Current state-of-the-art and future challenges,” IEEE Trans. Ind. Electron. vol. 62, no. 5, pp., May 2015.
[2] Z. Yang, F. Shang, I. P. Brown, and M. Krishnamurthy, “Comparative study of interior permanent magnet, induction, and switched reluctance motor drives for EV and HEV applications,” IEEE Trans. Transp. Electrific. vol. 1, no. 3, Oct. 2015.
[3] E. Bostanci, M. Moallem, A. Parsapour, and B. Fahimi, “Opportunities and challenges of switched reluctance motor drives for electric propulsion: A comparative study,” IEEE Trans. Transp. Electrific., vol. 3, no. 1, pp. 58– 75, Mar. 2017.
[4] J. Cai and Z. Deng, “Unbalanced phase inductance adaptable rotor position sensor less scheme for switched reluctance motor,” IEEE Trans. Power Electron., vol. 33, no. 5, pp. 4285–4292, May 2018.
[5] A. Chiba, K. Kiyota, N. Hoshi, M. Take-moto, and S. Ogasawara, “Development of a rare-earth-free SR motor with high torque density for hybrid vehicles,” IEEE Trans. Energy Converters., Mar. 2015.
[6] J. Ye, B. Bilgin, and A. Emadi, “An extended-speed low-ripple torque control of switched reluctancemotor drives,” IEEE Trans. Power Electron., Mar. 2015.
[7] W. Ding, S. Yang, Y. Hu, S. Li, T. Wang, and Z. Yin, “Design consideration and evaluation of a 12/8 high-

torque modular-stator hybrid excitation switched reluctance machine for EV applications," IEEE Trans. Ind. Electron., vol. 64, no. 12, Dec. 2017.

[8] C. Gan, J. Wu, M. Shen, S. Yang, Y. Hu, and W. Cao, "Investigation of skewing effects on the vibration reduction of three-phase switched reluctance motors," IEEE Trans. Magn., vol. 51, no. 9, Sep. 2015,

[9] M. A. Kabir and I. Husain, "Design of mutually coupled switched reluctance motors (MCSRMs) for extended speed applications using 3-phase standard inverters," IEEE Trans. Energy Convers., Jun. 2016.

[10] R. Martin, J. D. Widmer, B. C. Mecrow, M. Kimiabeigi, A. Mebarki, and N. L. Brown, "Electromagnetic considerations for a six-phase switched reluctance motor driven by a three-phase inverter," IEEE Trans. Ind. Appl., Sep./Oct. 2016.

[11] S. Song, Z. Xia, Z. Zhang, and W. Liu, "Control performance analysis and improvement of a modular power converter for three-phase SRM with Y- connected windings and neutral line," IEEE Trans. Ind. Electron., vol. 63, no. 10, Oct. 2016.

[12] S. Song, Z. Xia, G. Fang, R. Ma, and W. Liu, "Phase current reconstruction and control of 3-phase switched reluctance machine with modular power converter using single dc-link current sensor," IEEE Trans.

[13] F. Peng, J. Ye, and A. Emadi, "An asymmetric three- level neutral point diode clamped converter for switched reluctance motor drives," IEEE Trans. Power Electron., vol. 32, no. 11, pp. 8618–8631, Nov. 2017.

[14] A. K. Mishra and B. Singh, "Solar photovoltaic array dependent dual output converter based water pumping using switched reluctance motor drive," IEEE Trans. Ind. Appl., vol. 53, no. 6, pp. 5615–5623, Nov./Dec. 2017.

[15] F. Yi and W. Cai, "A quasi-Z-source integrated multiport power converter as switched reluctance motor drives for capacitance reduction and wide speed-range operation," IEEE Trans. Power Electron., vol. 31, no. 11, pp. 7661–7676, Nov. 2016.

[16] Y. Hu, C. Gan, W. Cao, C. Li, and S. J. Finney, "Split converter-fed SRM drive for flexible charging in EV/HEV applications," IEEE Trans. Ind. Electron., vol. 62, no. 10, pp. 6085–6095, Oct. 2015.

[17] Y. Hu, C. Gan,W. Cao, Y. Fang, S. J. Finney, and J.Wu, "Solar PV-powered SRM drive for EVs with flexible energy control functions," IEEE Trans. Ind. Appl., vol. 52, no. 4, pp. 3357–3366, Jul./Aug. 2016.

[18] C. Gan, J. Wu, Y. Hu, S. Yang, W. Cao, and J. M. Guerrero, "New integrated multilevel converter for switched reluctance motor drives in plug-in hybrid electric vehicles with flexible energy conversion,"IEEE Trans. Power Electron., vol. 32, no. 5, pp. 3754– 3766, May 2017.

[19] M. Amiri, H. Farzanehfard, and E. Adib, "A nonisolated ultrahigh step down dc–dc converter with low voltage stress," IEEE Trans. Ind. Electron., vol. 65, no. 2, pp. 1273–1280, Feb. 2018. .